FULL AUTHORITY ACTIVE CONTROL SYSTEM DESIGN FOR A HIGH PERFORMANCE HELICOPTER

D Walker and I Postlethwaite
Department of Engineering
University of Leicester
Leicester LE1 7RH, U.K.

Abstract

We report on a continuing study into the application of H^∞ optimal control theory to the design of a low-speed full authority active control law for a generic high-performance single main rotor helicopter. Two new designs are presented, each based on an eight state linearization of a non-linear helicopter model provided by the Royal Aerospace Establishment, Bedford. Both designs have the same structure. An inner loop feeds rate and attitude signals directly back to respective activators, in a manner reminiscent of some auto stabilization schemes in use. An outer loop then feeds back the controlled output measurements to a dynamic controller designed using H^∞ optimization. The use of the inner loop helps relieve the task of robust stabilization faced by the outer loop, by providing a simple and direct improve-ment to the unaugmented vehicle's stability. It also makes the process of design of the second loop simpler, and yields a lower order controller. Further-more, such a scheme offers the advantages often associated with a decentralized controller. We offer an appraisal of both control laws in the low speed flight regime for which they were designed.

1. INTRODUCTION

The high levels of non-linearity and the cross-coupling characteristic of a typical single rotor helicopter make the task of active control law design difficult. It is however widely believed that some form of augmentation is necessary to ease pilot workload, and meet stringent handling quality specifications. In situations where high performance and agility are required this is particularly so. Given this interactive nature, it is natural to look to multi-variable control system theory to provide a solution to the control problem. In so doing, the important issues of robustness and uncertainty need to be considered in order to arrive at designs which are satisfactory. In this paper, we shall present some results of work under-taken to apply H^∞ optimal control theory to problems relating to helicopter control.

Let us explain in brief what is meant by uncertainty, and what a robust control system is. Taking the latter first, it is often the case that when a controller is designed, the exact values of parameters describing the system to be controlled are not precisely known. Even the very workings of the system may not be completely understood, or at least not readily quantifiable. Obviously, if a controller is to be satisfactory, it must be capable of accommodating both changes occurring within the system itself, and any departure of the behaviour of the latter from the assumed behaviour on which the controller design was based. A controller which performs satisfactorily in the face of such variations is said to be robust.

Uncertainty is a collective term referring to the effects arising from the imprecise or non-inclusion to the model of any factors which affect, or are part of, the real system. Such may be as a result of ignorance, or as a result of deliberate choice: e.g. in the case of using a linearized model to approximate the behaviour of a non-linear system in the region of an operating point, the benefits afforded by the use of linear techniques may justify the deliberate introduction of 'imprecision'. Bearing in mind that in most engineering cases, the non-linear model itself is only to be regarded as an approximation, this seems not unreasonable.

The designs we have performed were all based on linearized models taken from the Rationalized Helicopter Model (RHM14) supplied by RAE Bedford; as a linearized model was used the issue of uncertainty clearly must be considered. Furthermore, the RHM14 did not include a dynamic model of the rotors, thus introducing further uncertainty into the problem also, the designs we performed were based on a model in which the engine dynamics were not simulated. We chose to use a reduced order eight state model, thus ignoring actuator and other states. This we did to simplify the design and to reduce the state dimension of the final controllers. As will be shown in section four, enough robust-ness was built into the designs that those uncertainties could be accommodated without detriment to stability.

H^∞ Optimal Control

As interest in robust control design has increased a substantial portion of the literature has been concerned with H^∞ optimization techniques. Although solution methods have been available since the early 80's, recent theoretical developments have brought about significant improvements in the solution algorithms, which have enabled dramatic improvements from a numerical/ computational point of view [1,2]. Numerous applications of the theory to design problems have been reported[3, 4].

In recent work on the helicopter control problem, Yue and Postlethwaite demonstrated that H^∞ control theory could be applied to yield a fixed parameter controller giving good performance in the low speed regime, as well as good robust stability over an extended range of flight conditions. A low speed controller which they had developed was tested in real-time in a flight simulator at RAE Bedford where, even when run into the high speed range, the test pilot reported that the controller made the helicopter more pleasant to fly than the open loop (uncontrolled) helicopter.

It was however recognised that the deterioration in performance exhibited by the low speed controller as speed increased would need to be overcome by a future full authority active control law. There are various means by which this might be achieved.

Aims of this paper.

We present two 16 state H^∞ -suboptimal low speed controllers which have been developed as part of our investigation into how the 'effective performance radius' of a single fixed parameter controller can be increased. We have used two distinct H^∞ optimization methods to derive the controllers. These will be further explained in section two. Both designs are two stage. The first stage consists of constructing inner attitude and rate feedback loops. We then use the same inner loop in both designs, whose second stages consist of H^∞ robust stabilizations with additional performance constraints built in.

Both designs we analyse, in linear time and frequency domain as well as on the non linear RHM14 model. Using a proposed American military specification of handling qualities [5], we offer an appraisal of the closed loop properties.

The remainder of the paper is laid out as follows: In section 2 we outline the main points of the two H^∞ design methods of interest. A description of the helicopter model is given in section 3, together with a definition of the type of control required. The main results are presented in section 4, in the form of a description and an analysis of the designs, and in section 5, where a handling qualities evaluation is made on the basis of non-linear computer simulations.

2. Two H^∞ Design Methods

The basic aim of the control law will be to achieve simultaneous robust performance and stability in the face of disturbances, parameter variations, unmodelled dynamics etc. We shall now recapitulate some of the results and methods relating to H^∞ theory which will be used in our work. A good introduction to the subject is given by Francis [6].

Generally, problems in robust design involve a compromise between performance and uncertainty. In standard H^∞ designs this trade off is usually embodied in a compound performance index, which can be used to bound functions which regulate both performance and robustness. The first design which we present uses this formulation in its simplest useful form; we formulate the problem as a weighted sensitivity and robustness problem, some-times called weighted S,KS. Consider the feedback arrangement solution in Figure 1.

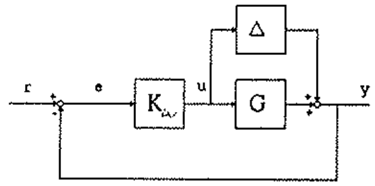

Figure 1

The aim of the γ-suboptimal weighted S,KS problem is to find a stablizing controller K which also achieves

$$\left\| \begin{matrix} W_1 (I+GK)^{-1} \\ W_2 K(I+GK)^{-1} \end{matrix} \right\|_\infty \leq \gamma \qquad (2.1)$$

Here W_1 and W_2 are frequency dependent weighting functions supplied by the designer. The basic motivation behind such a performance index is as follows: Note that

$$T_{er} = -T_{ed} = (I+GK)^{-1} \qquad (2.2)$$

$$T_{ur} = -T_{ud} = K(I+GK)^{-1} \qquad (2.3)$$

where, for example, the transfer function from r to e is denoted by T_{er}. For any stabilizing K satisfying (2.1), we have that

$$\bar{\sigma}(T_{er}) = \bar{\sigma}(T_{ed}) \leq \gamma\bar{\sigma}(W_1^{-1}) \qquad (2.4)$$

$$\bar{\sigma}(T_{ur}) = \bar{\sigma}(T_{ud}) \leq \gamma\bar{\sigma}(W_2^{-1}) \qquad (2.5)$$

Thus, by judicious choice of the weighting functions W_1 and W_2 upper bounds can be placed on the singular values of these four transfer functions at any frequency. For example, making $\bar{\sigma}(T_{er}) \approx 0$ at low frequencies, say $0 < \omega < \omega_1$, would have the effect of making the D.C. error of the system small. However, trying to force too much bandwidth by prescribing too large a W_1 would start to increase the controller bandwidth and thus cause problems of robustness, implementation, noise etc. Therefore, by ensuring W_2 is 'large' at frequencies above the desired control bandwidth ω_{B1} the energy content of the control signal u can be kept down. Referring to Fig. 1, and eqn. 2.3 it will be seen that minimizing the energy gain to the signal u also optimizes robustness with respect to unstructured additive perturbations Δ to the nominal plant G.

Having decided on the form (2.1) of the cost functional, the design becomes a matter of selecting appropriate weights W_1 and W_2. This usually involves trial and error. We mention in passing that the solution to the problem associated with 2.1 also generally requires iteration, there being no direct way of calculating the minimum γ for which a solution exists. Nontheless, reliable methods exist to enable optimal or suboptimal solutions to be obtained using standard techniques from linear algebra. The McMillan degree of the controller is in general of similar order to the combined degree of nominal plant plus weights.

Loop shaping design procedure

Our second design uses the loop shaping design procedure based on the normalized left coprime stable factor perturbation model developed at Cambridge by McFarlane and Glover [7, 8]. This design procedure consists of first selecting pre and/or post dynamic compensators W_1 and W_2 for the open loop plant G which shape the open loop forward path transfer function $G_s = W_2 G W_1$ (Recall that an inner loop feedback stabilization has already been performed). See Figure 2a. This loop shape will in general embody the requirement for high gain at D.C. and low frequencies for low steady state error, whilst forcing a low gain at high frequencies in order to control the bandwidth, and for considerations of robustness to higher-frequency model errors. The loop shape may also be chosen so as to modify the roll off rate in the vicinity of the cross over frequency, which can help with the resulting system's stability margins. Thus far, no consideration of stability is made. Having constructed the desired loop shape, the robust stabilization process which follows returns a

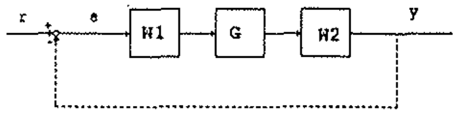

Figure 2a

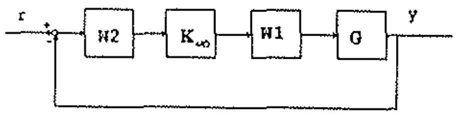

Figure 2b

controller which stabilizes the shaped plant. In doing so, the original loop shape will be altered by the inclusion of the controller K_∞ into the loop (see Fig. 2b). However, bounds have been given for the degradation, and provided the levels of performance and robustness demanded by the original loop shape are reasonably compatible with the open loop plant's characteristics, then the degradation has been shown to be small.

The stabilization process actually robustly stabilizes the shaped plant to perturbations on its normalized coprime factors. Such models of uncertainty have been studied by Vidyasagar

[9], Georgiou & Smith [10]. It has been shown that they offer certain advantages over the more common additive or multiplicative models often used. For example, the latter two do not allow for uncertainty in number of unstable poles in the system; likewise, when there exist poles with lightly damped resonances whose position is uncertain, the normalized coprime factor approach offers advantages as a means to model this as a norm bounded perturbation. A tutorial introduction to the method is given by Glover et al [11] . Finally it should also be noted that McFarlane and Glover showed that this formulation leads to an optimization problem which has a closed form solution. Thus no iteration is required to calculate the controllers which give optimal robustness properties, and the design procerss is consequently much faster. This makes the design procedure very attractive.

3. Helicopter Model and Control Law Type

The non-linear model used for the work is the Rationalized Helicopter Model (RHM14) provided by RAE Bedford. This is a non-linear simulation of a generic single main rotor helicopter, and is essentially the same as the model which is used on the Bedford flight simulator. It runs from within the TSIM environment. The model consists of numerous modules which calculate and simulate aerodynamic forces, moments, actuators etc., at a chosen flight condition. It is possible to modify the flight condition and trim the aircraft about a desired operating point. The TSIM language allows linearizations to be taken at such operating points. The RHM14 included no rotor dynamic models, and when the original designs were performed, the engine module was not run with the model for technical reasons. However, in previous work on a similar problem, Yue and Postlethwaite had deliberately opted to treat the rotor dynamics as uncertain, and had found that by limiting the bandwidth the effects of rotor-dynamic uncertainty could be suppressed and were not detrimental[3, 4]. For present purposes, we shall ignore actuator dynamics from the linear designs. These are mödelled in the RHM14 as first order tags with rate and ampitude limits. Finally a control law interface has been developed at RAE which has enabled the controllers designed to be evaluated back on the non-linear model [12].

Low speed controller.

Our aim was to design a controller for the low speed range, where it was considered that an attitude command attitude hold system was most appropriate.

Two linearizations of the equations of motion were made at one knot. The first linearization had eight states. It can be expressed in standard state space form as

$$\dot{x} = Ax + Bu$$
$$y = Cx$$

where

$$x = [\theta\ \phi\ p\ q\ r\ u\ v\ w]^t$$
$$u = [\theta_o\ \theta_{ls}\ \theta_{lc}\ \theta_{ot}]^t$$
$$y = [\dot{h}\ \theta\ \phi\ \dot{\psi}]^t$$

see tables 1, 2, 3 below. (A nine state model with state ψ (the yaw angle) was discarded on the grounds that it led to similar results, at the cost of increased numerical difficulties and higher final state dimensions). The eight state model was used for the designs.

State	Description	Units
θ	pitch attitude	rad
ϕ	roll attitude	rad
p	roll rate	rad s^{-1}
q	.pitch rate	rad s^{-1}
r	yaw rate	rad s^{-1}
u	forward vel	ft s^{-1}
v	lateral vel	ft s^{-1}
w	downward vel	ft s^{-1}

Table 1

Input	Description	Units
θ_o	main rotor collective	deg
θ_{ls}	longitudinal cyclic	deg
θ_{lc}	lateral cyclic	deg
θ_{ot}	tail rotor collective	deg

Table 2

Controlled Output	Description	Units
$\dot{h}$	heave vel	ft/sec
θ	pitch attitude	rad
ϕ	roll attitude	rad
ψ	heading rate	rad/sec

Scaling	Pilot Input
10	coll
0.2	long
0.5	LAT
0.5	PEDAL

Table 3

The open loop model is unstable and poorly conditioned. (DC condition no. = 1285) see Fig. 4.

The use of scaling given in Table 3 on the outputs was suggested in [3]. This helps to improve the numerical conditioning of the H^∞ optimization.

The controllers were designed with the aim of robustly stabilizing the system, and providing as much decoupling between the contracted outputs as possible. Thus, for example, a unit pilot input on coll should produce a 10 ft/sec change in heave velocity, with minimal change in heading rate, roll or pitch attitude.

4. RESULTS OF CONTROLLER DESIGN

The overall control scheme consisting of inner and outer loops is shown schematically in Fig. 3. The controller K_∞ is dynamic and will be obtained via H^∞ optimal methods. It forms an outer control loop.

Inner Feedback Loop

In order to improve the stability of the vehicle prior to the H^∞ robust stabilization, three inner feedback loops were made. These are represented by the constant feedback selection matrix F shown in Fig. 3, within the inner loop.

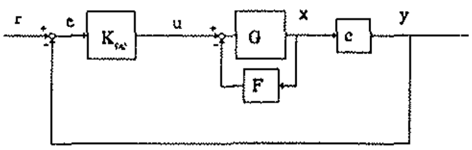

Figure 3

The main effect of this is to stabilize the unstable mode which is basically a pitching mode. Also the roll and yaw axis feedback helps to improve the damping of the final closed loop. After some experiment, the gains were set to the values given in table 4. These gains were used in both designs.

axis	feedback signal	gain	fed back to
pitch	θ	0.4 deg/deg	θ_{ls}
	q	0.2 deg/deg/sec	θ_{ls}
roll	ϕ	-0.2 deg/deg	θ_{lc}
	p	-0.1 deg/deg/sec	θ_{lc}
yaw	r	-0.2 deg/deg/sec	θ_{ot}

Table 4

The pole positions of the compensated and uncompensated plant are given in Table 5

	Poles
uncompensated	-11.41
	- 2.29
	0.23 ± 0.54
	- 0.20 ± 0.59
	- 0.63
	- 0.52
compensated	-26.38
	-13.37
	- 5.65
	- 1.78
	- 0.07 ± 0.08
	- 0.50

Table 5

The outer loop design can now be performed. This will give the dynamic controller K_∞, whose inputs will be the errors on each of the four outputs which are to be controlled.

4.1 Design 1

Design 1 is a weighted S,KS design. We chose W_1 so as to ensure low steady state error in all channels as well as a satisfactory dynamic response. After some trial and error, we eventually used the following W_1 :

$W_1(s) =$

$$\begin{Bmatrix} \frac{.1(s+12)}{(s+.012)} & & & \\ & \frac{.178(s+8.43)}{(s+.015)} & & \\ & & \frac{.178(s+8.43)}{(s+.015)} & \\ & & & \frac{.1(s+10)}{s+.01} \end{Bmatrix}$$

The second weight W_2 has to embody constraints on control effort and bandwidth arising out of actuator performance limits and robustness considerations. Yue and Postlethwaite had shown using a non-linear helicopter model Helisim (which had a rotor dynamic model) that rotor blade uncertainty became important at above 10 rad/sec. With this in mind, together with an estimate of the available actuator bandwidth, we eventually settled on the following value for W_2

$$W_2(s) = \frac{0.1(s+0.0001)}{(s+10)} I_4$$

The weights' frequency responses are shown in Fig. 5. Having formulated the optimization, it was found that the optimal controller had 15 states, and that the optimal cost, $\gamma opt = 0.617$. However, in order to obtain a strictly proper controller, we used a suboptimal $\gamma = 1$ for the final design. The sensitivities and robustness functions are shown below. (Figs. 6, 7, 8). Also shown are singular value plots of the forward path transfer function GK and the controller K (Figs. 9, 10). The optimization has introduced high gain at low frequency, which rolls off at a little beyond 4 rad/sec. From the plot of $\bar{\sigma}_i$ $(I + KG)^{-1}$ it can be deduced that the gain and phase margins for each input channel are approximately

GM (3.42, .59)
P.M. $\pm$ 41.5^o

These margins are probably pessimistic as the unstructured singular $\sigma(\cdot)$ tends to give conservative results. Indeed, where information is available as to the structure of the uncertainty, the structured singular value μ is a more appropriate tool.

Linear time simulation.

Fig. 11 shows the response of the closed loop helicopter to step demands input on each of the four pilot controls. The corresponding control actions are shown in Fig. 12.

The control action remains within the saturation limits of the actuators and the performance appears to be good. The goal of reducing the interaction between the four axes has also been successful.

Non-linear time simulation.

Responses are shown to step demands on each of the four pilot controls. The non-linear responses do not differ significantly from the linear responses above. Using the control law interface provided by RAE, the controller was linked to the RHM14 model. (Figs. 13, 14, 15, 16).

Design 1, non-linear time simulation

Responses are shown for the respective output and actuator responses (Figs. 13-16). It was noted that the pitch, roll and yaw axes responded in virtually the same way as they had on the linear simulation. The heave axis had however become a good deal more sluggish in its response when compared with the linear responses (Fig. 11). This degradation is due to the omission of engine dynamics from the linear model which was used for the design; the RHM14 model used in the non-linear evaluation presented in this paper incorporated a fully working engine-dynamic model.

DESIGN 2

We now describe the loop-shaping/ normalized left coprime factor robust stabilization design. This was also performed on a 1 knot linear model, and the design aims were the same as those of the first design. We used the same inner feedback structure with identical gains. The loop-shaping design was carried out on the squared-down system, whose inputs were the errors associated with each of four controlled outputs. The pre- compensator $W_1(s)$ (see Fig. 2a) was chosen with the simplest dynamics which yielded satisfactory results. It consisted of integral action in each of the four channels, followed by an alignment Ka, which is simply a constant matrix, followed by a further constant diagonal gain which was used to boost the gains differentially in each channel. The choice of W_1 is shown in Fig. 17. The weight has forced the basic shape required to obtain low steady state error, whilst providing a steady roll-off of gain at higher frequencies which is required for robustness, as well as to eliminate noise problems, controller bandwidth problems and so on. Having chosen this loop shape, the robust stabilization stage of the design was performed. The resulting controller had a state dimension 15. (The optimization leads to a controller for the shaped plant with one fewer state than the shaped plant. This controller is then cascaded with shaping weights W_1 and W_2 (see Fig. 2b) in order for it to control the original unshaped plant). The optimal cost associated with the optimization was γ=2.2258, small enough to ensure a satisfactory stability margin $\varepsilon = 1/\gamma = 0.449$ with respect to perturbations on the normalized coprime factorization. (N.B. The stability margin ε can only lie in the range $0 < \varepsilon < 1$). McFarlane and Glover have shown that the closer the value of ε is to the value 1, the less is the degradation caused to the chosen loop shape by the introduction of robust controller. Thus, a small value of the implies that the required loop shape can be accommodated with a good degree of robust stability.

We performed the design at the slightly suboptimal value of γ=2.3. This led to a strictly proper controller KINF with a state dimension of 16. The actual loop shape obtained when this controller was introduced into the loop is shown in Fig. 18. Comparison with the candidate loop shape (Fig. 17) confirms that the basic shape remains little altered.

Design 1, Linear Evaluation

The output responses of the closed loop linearized system to step demands on each of the pilot controls are shown in Fig. 21. (Recall that the outputs are scaled in accordance with Table 3, section 3). It was noted that a slight overshoot characterized the responses to step demands of heave velocity and pitch and roll attitude; however, these phenomena were not considered to be a serious defect. By pre-filtering the respective pilot demands with a first order lag of time constant 0.5 sec it was found that the over-shoots could be virtually eliminated without significantly affecting performance. The respective control actions are shown in Fig. 12. The actuator rate and amplitude behaviour is within provisional limits.

From Fig. 20, the following gain and phase margins for each input channel can be deduced:

G.M. = (1.11, 0.909)
P.M. = ± 5.7 deg

It would thus appear that the stabilization procedure has, whilst providing near optimal robustness with respect to stable factor perturbation, yielded poor gain and phase margins. However, we caution against interpreting these margins as evidence of lack of robustness of the design, reminding instead that gain and phase margins can, in the multivariable scenario, lead to extreme conservatism.

Design 2, Non-linear evaluation

The step responses of the controlled helicopter as predicted by the non-linear simulation are shown in Figs. 23-26. As in design 1, the major difference is a deterioration in heave axis performance which is due to the presence of the engine model. The response of pitch, roll and yaw axes have however maintained virtually the same characteristics as in the linear simulation, showing low levels of cross coupling, and responses which appear good.

Robustness of the designs

Comparison between the linear and non-linear time responses confirms that both the designs were robust to the uncertainties introduced by the use of a linearization for the control law design. The additional presence of engine dynamic uncertainty, whilst causing some performance deterioration, was nevertheless accommodated by both designs. Regarding the question of rotor dynamic uncertainty, in this present study we have not been able to make a comprehensive assessment of its impact on the robustness and stability of the two designs. However, we believe, on the basis of studies by Yue and Postlethwaite [3], that control problems relating to rotor dynamic uncertainties can be overcome by forcing bandwidth constraints (Figs. 8, 9, 18).

Finally, we consider a phenomenon arising out of the use of linear perturbation model to approximate a non-linear system. The extent to which changes in the perturbation model with forward speed affect the performance of a given controller is a key issue in determining the effective performance radius of that controller. However, if the controller is to be used in a regime other than that for which it was designed by treating that regime as a perturbation about the design point, any robustness which it has to parameter variations in perturbation model due to change in flight condition may be lost as a result simply by being too far from the nominal flight condition. This may cause much greater deterioration in performance than would result if the controller could be trimmed-in at the new operating point.

The time responses show in Figs. 13-16 and 23-26 were obtained by trimming in the controllers to the non-linear model at 1 knot. We performed the same tests on the controllers trimmed in to the model at various speeds up to 50 knots. The results showed that once the controller was trimmed-in it provided good control even far away from its design region. This has led us to conclude than an important feature required to enable the performance radius of a single controller about its design point to be mazimized is some form of trim scheduling, which would help overcome the effects of non-linearity and varying nominal values.

5. HANDLING QUALITIES EVALUATION

In this section, we assess the handling qualities afforded to the helicopter by each of the control laws described in section four. We do so by analysing appropriate time histories obtained from the non-linear simulation, using performance criteria laid down in a "Proposed Specification for Handling Qualities of Military Rotorcraft" [5].

The criteria given in this document are intended to go some way at least towards quantifying the behaviour of rotorcraft, and to enable objective statements to be made about their handling qualities. The specifications given primarily define desirable levels of aircraft response to pilot inputs and state values for acceptable inter-axis coupling. For more detailed discussion of handling qualities, see [5].

We offer an evaluation of both control laws based on the following:

i) heave axis response to collective
ii) heave to yaw coupling
iii) pitch axis response
iv) roll axis response
v) pitch to roll coupling
vi) roll to pitch coupling

1) Small amplitude pitch and roll attitude changes: Short Term Response

We evaluate the bandwidth and phase delay parameters defined in Fig. 2 (3.3) of the specification in order to classify the short term responses of the pitch and roll axes. Out of necessity, the appropriate frequency domain parameters were obtained by analysing a series of time responses from the non-linear simulation. The bandwidth and phase delay parameters τ_P and Ω_{BW} for both designs are plotted in Fig. 27, onto which boundaries are superimposed demarking the various handling quality classifications. Both designs are within the level 1 region.

2) Inter-axis coupling: Pitch-to-roll and roll-to-pitch coupling during aggressive manoeuvring

For an attitude response type, the specification lays down that the ratio of peak off-axis response ($\theta_{peak}/\phi_{step}$ or $\phi_{peak}/\theta_{step}$) must be < 0.25 (< 0.65) for classification as level 1 (level 2). We tested each design with three step demands of 10, 20 and 30 degrees on roll and pitch axes. The greatest coupling induced was 5 deg peak pitch to a step of 30 deg on roll; both designs were comfortably within the level 1 region.

3) Collective induced yaw

With the design 1 controller, a step demand in heave velocity induced a maximum yaw rate of approximately 4 deg/sec. Furthermore, it was found that larger amplitudes heave-velocity step demands caused proportionately higher induced yaw rates. The design 2 controller caused a lower maximum induced yaw rate of approximately 2 deg/sec. However, it was also found that the situation worsened at higher heave velocity demands. These resuls are shown in Fig. 28. Design 1 is level 2, and design 2 is borderline level 1/2.

4) Height response to collective

"The vertical rate response following a step collective input shall have a qualitative first-order appearance, given by

$$\frac{\dot{h}}{\delta c} = \frac{K\, e^{-\Delta s}}{1+ST}$$

The limits on Δ and T are given by

level	T	Δ
1	5	0.2
2	∞	0.3

The approximate parameters for each design were found to be

Design 1 $T = 1.5$ sec
$\Delta = 0.3$ sec
Design 2 $T = 1.44$ sec
$\Delta = 0.2$ sec

Thus, owing to the relatively large effective time delays present, both designs only satisified level 2 in this test.

6. CONCLUSIONS

Two attitude-command attitude-hold low speed control laws have been presented, each designed by a separate H^∞ optimization procedure. Both designs were configured so as to ensure robustness to modelling error and parameter variation due to changing flight condition.

The use of an inner loop consisting of constant gains feeding back attitude and rate signals has been proposed. The importance of the rates in achieving good control and decoupling has been seen. In performing these designs, it has been found that it is more difficult to achieve good control by forming an inner rate/attitude feedback followed by a H^∞ optimization than it would have been to feed all the signals directly back to a suitably designed H^∞ controller. However, the inner loop feedback structure used in this paper offers the advantages of simpler weighting function selection in the S,KS design as well as a lower state order of the final controller. The use of this basic structure, with alternative inner-loop feedback schemes, remains a topic of research.

The presence of the engine model in the final non-linear tests demonstrated that both designs were robustly stable. However, there was a price to pay for this, primarily in terms of heave axis response. We aim to re-design both controllers using updated linearization. Otherwise, both designs achieved good robust stability and fairly good performance and decoupling.

7. ACKNOWLEDGEMENTS

This work has been carried out with the support of the Procurement Executive, U.K. MOD. We should like to thank several people at RAE, Bedford. However, particular thanks are due to J Howitt and P Smith for many helpful discussions and suggestions. Finally, we point out that any opinions expressed herein are those of the authors and are not necessarily shared by RAE.

REFERENCES

[1] J. Doyle, K. Glover, P. Khargonaker & B. Francis, "State space solutions to standard H^2 and H^∞ control problems", IEEE Trans. Auto. Control, 34(8), 831-848, August 1989.

[2] K. Glover, D. Limebeer, J. Doyle, E. Kasenally & M. Safonov, "A characterization of all solutions to the four block general distance problem", Accepted for publication, SIAM Journal of Control and Optimization.

[3] A. Yue & I. Postlethwaite, "Improvement of helicopter handling qualities using H^∞ optimzation", IEE Proc., vol. 137 Part D, No. 3, May 1990.

[4] A Yue, "H^∞ design and the improvement of helicopter handling qualities", D. Phil thesis, University of Oxford, 1988.

[5] R. Hoh, D. Mitchel, B. Aponso, "Proposed specification for handling qualities of military rotorcraft", Systems Technology Inc.

[6] B. Francis, "A course in H^∞ control theory", Lecture notes in Control and Information Science, Springer-Verlag, 1987.

[7] D. McFarlane, "Robust controller design using normalized coprime factor plant descriptions", Ph.D thesis, University of Cambridge, 1988.

[8] D. McFarlane & K. Glover, "An H^{∞} design procedure using robust stabilization of normalized coprime factors", Proc. 27th CDC, Austin, Texas, 198?

[9] M. Vidyasagar, "Control system synthesis: A factorization approach", MIT Press, 1985.

[10] T. Georgiou & M. Smith, "Optimal robustness in the gap metric", IEEE Trans. AC-35(6), 673-686, 1990.

[11] K. Glover, J. Sefton & D. McFarlane, "A tutorial on loop shaping using H^{∞} robust stabilization", to be presented at IFAC World Conference, Tallinn, Estonia, 1990.

[12] J. Howitt, "Proposed control law interface for the Rationalized Helicopter Model", draft copy of internal RAE document.

FIGURES

UNCOMPENSATED OPEN LOOP PLANT

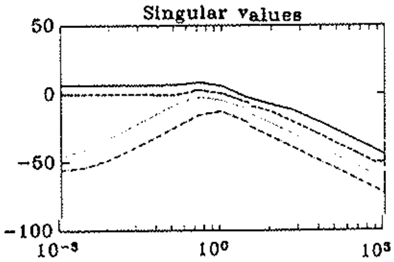

fig 4

DESIGN 1

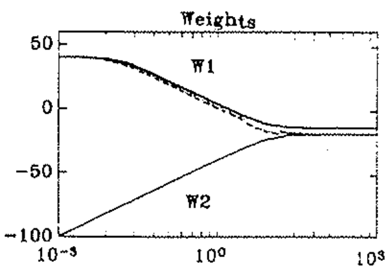

fig 5

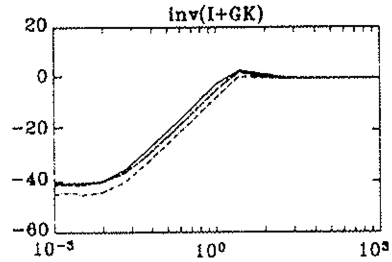

fig 6

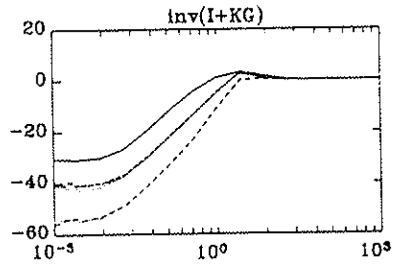

fig 7

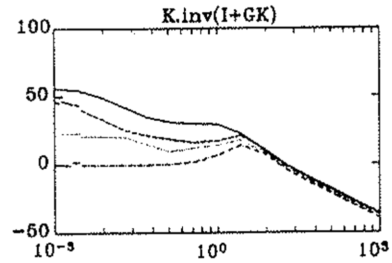

fig 8

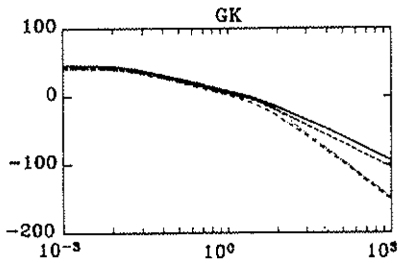

fig 9

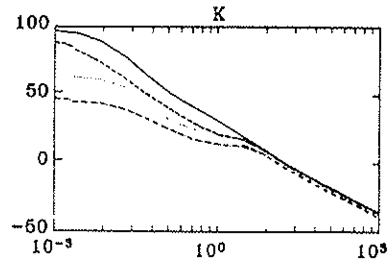

fig 10

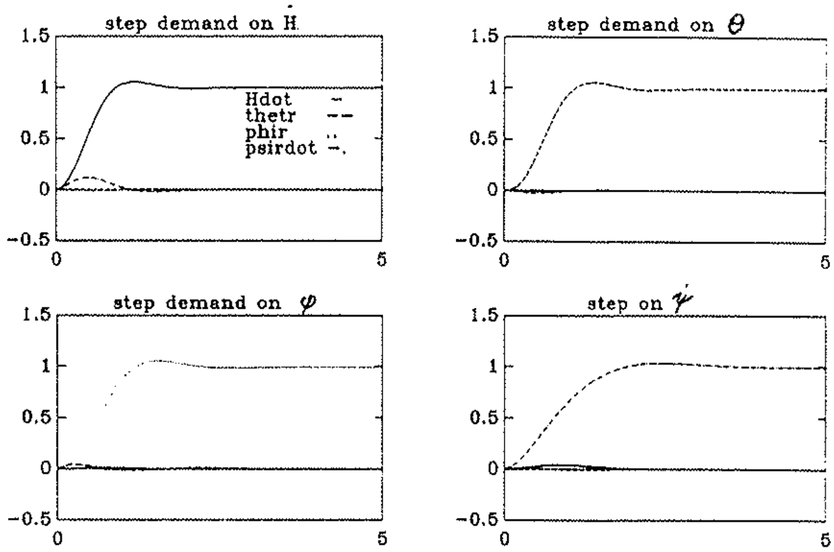

fig 11

DESIGN 1

LINEAR TIME RESP.

Scaled outputs

Ḣ 10 ft/s
θ 0.2 rad
φ 0.5 rad
ψ̇ 0.5 rad/s

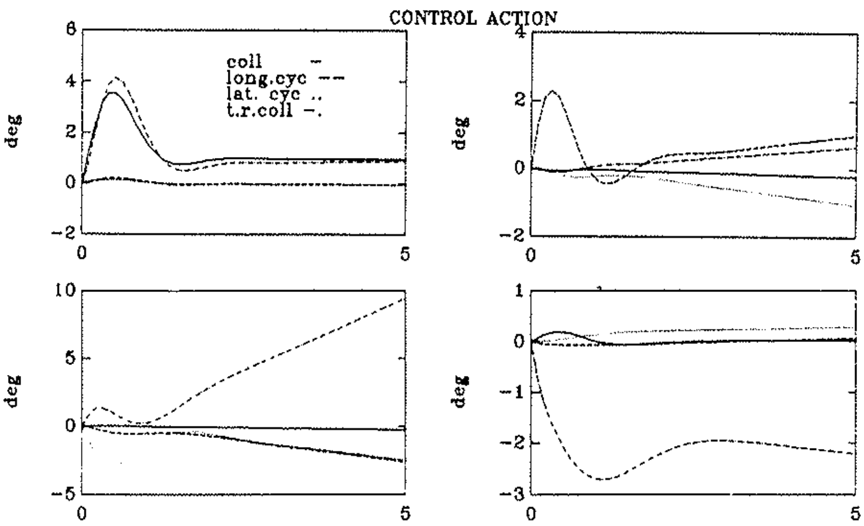

fig 12

HANDLING QUALITIES EVALUATION

fig 27 SHORT TERM RESP (PITCH & ROLL)

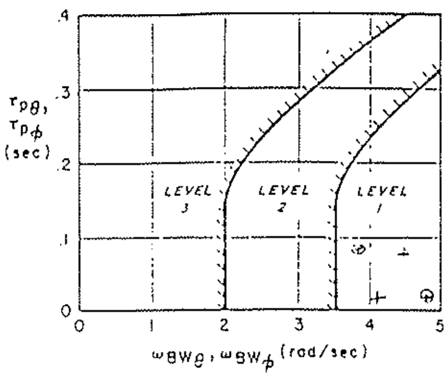

a) Target Acquisition and Tracking (pitch and roll)

COLL. INDUCED YAW

fig 28

⊕ Design 1

\+ Design 2

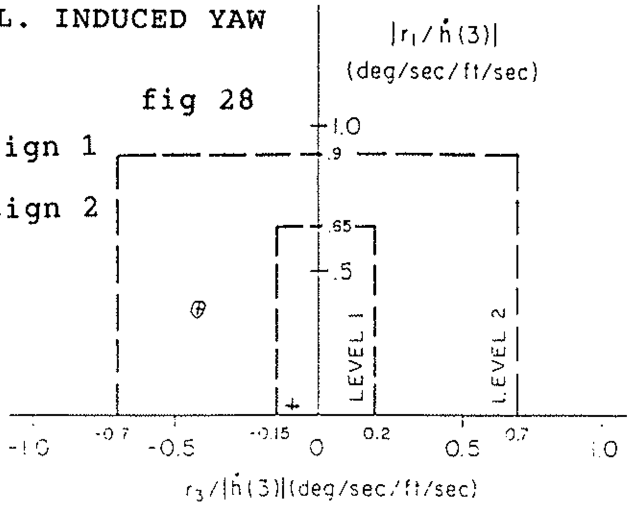

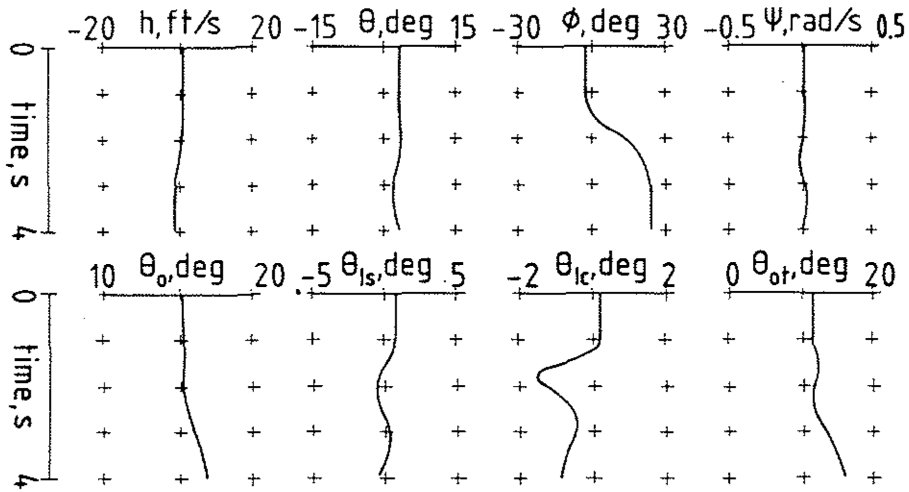

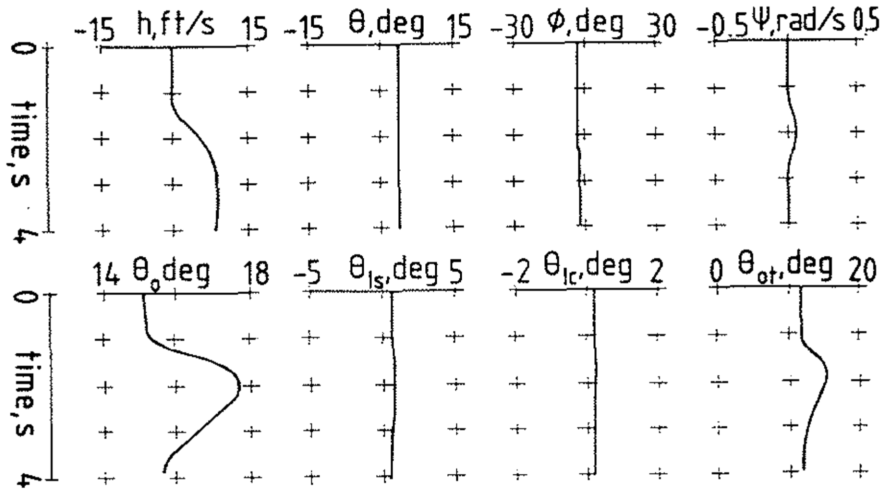

DESIGN 1

NON-LINEAR

TIME RESP.

fig 13-16

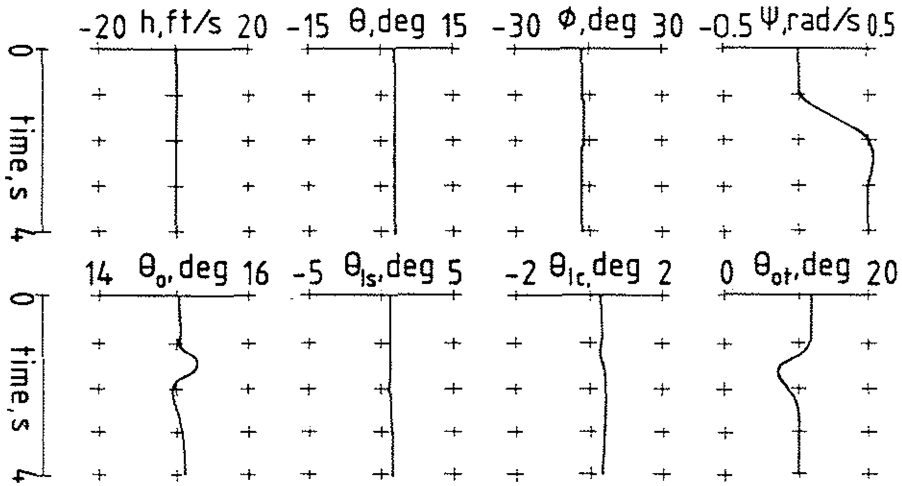

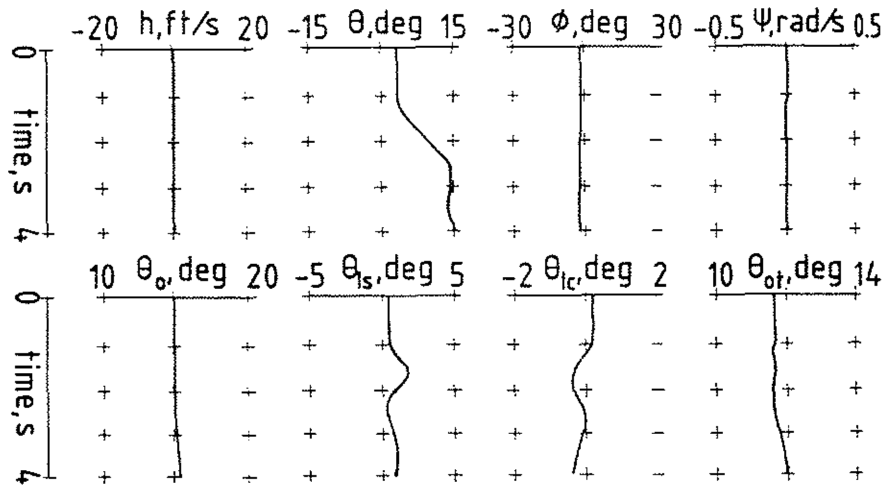

DESIGN 2

LINEAR FREQ. & TIME RESPONSES

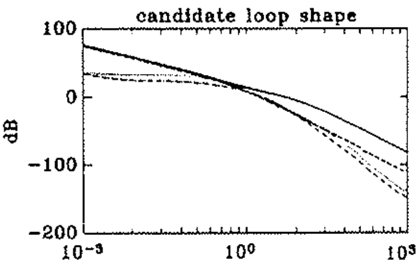

fig 17

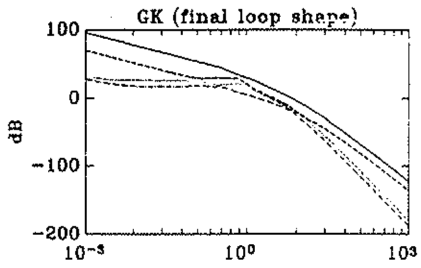

fig 18

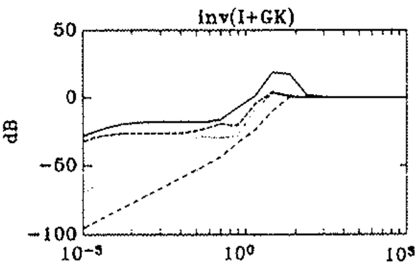

fig 19

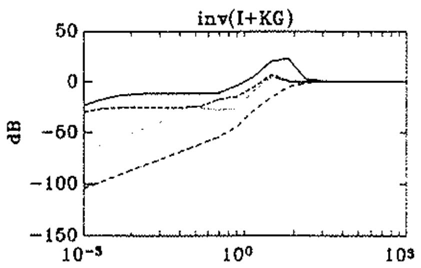

fig 20

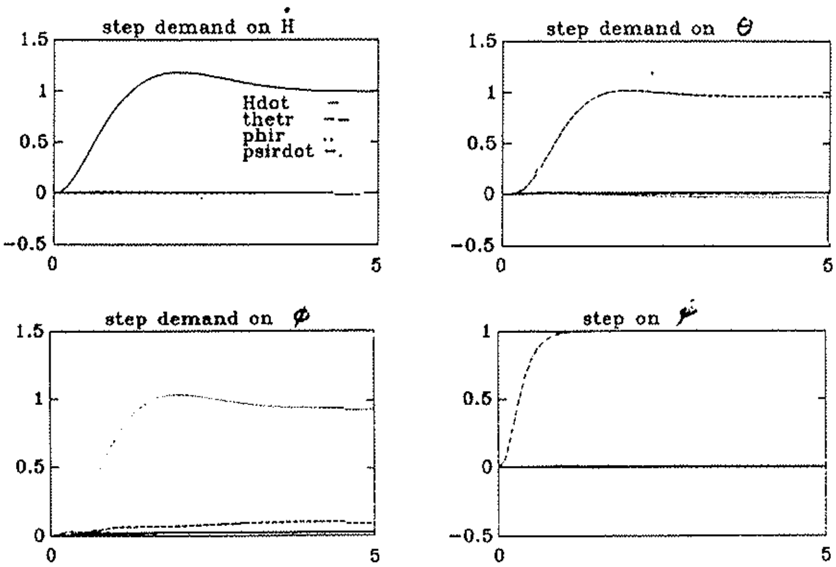

fig 21

Scaled outputs

$\dot{H}$	10	ft/s
θ	0.2	rad
ϕ	0.5	rad
$\dot{\psi}$	0.5	rad/s

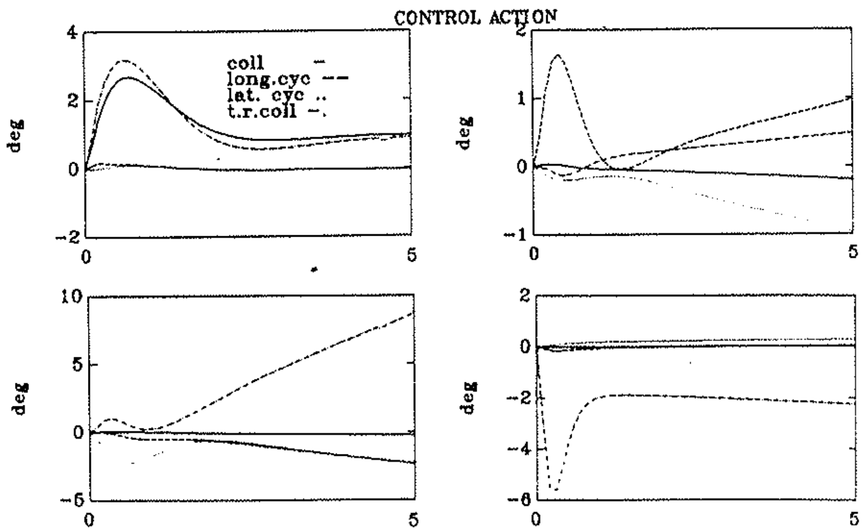

fig 22

DESIGN 2

NON-LINEAR

TIME RESP.

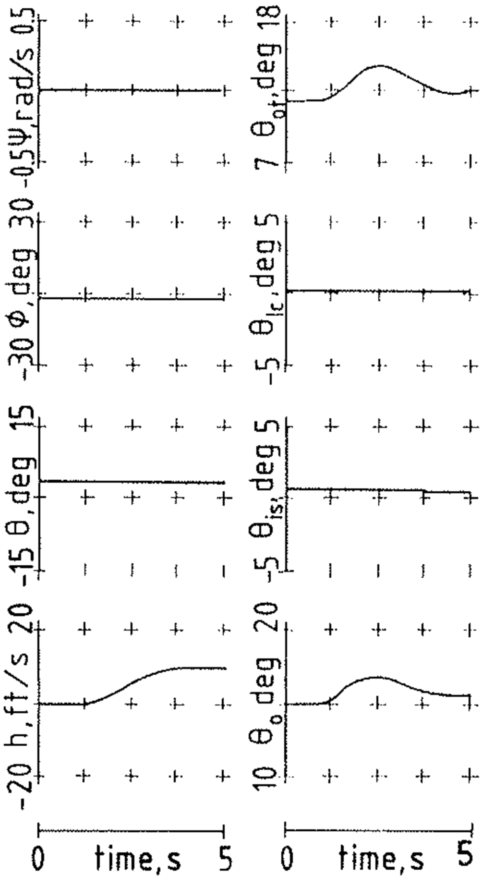

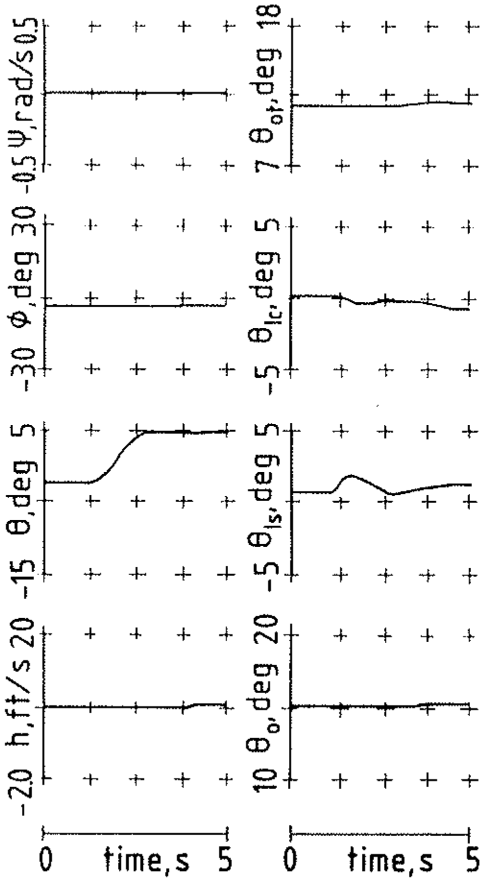

fig 23-26